

Cover Page



Universiteit Leiden



The handle <http://hdl.handle.net/1887/37233> holds various files of this Leiden University dissertation

Author: Tummers, Bart

Title: Human papillomavirus targets crossroads in immune signaling

Issue Date: 2016-01-21

4

The interferon-related developmental regulator (IFRD1) is used by Human papillomavirus (HPV) to suppress NFκB activation

Tummers B, Goedemans R, Pelascini LPL, Jordanova ES, van Esch EMG, Meyers C, Melief CJM, Boer JM, van der Burg SH.

Nat Commun. 2015 Mar 13;6:6537.

ABSTRACT

High-risk human papillomaviruses (hrHPVs) infect keratinocytes and successfully evade host immunity despite the fact that keratinocytes are well equipped to respond to innate and adaptive immune signals. Using non-infected and freshly established or persistent hrHPV-infected keratinocytes we show that hrHPV impairs the acetylation of NF κ B/RelA K310 in keratinocytes. As a consequence, keratinocytes display a decreased pro-inflammatory cytokine production and immune cell attraction in response to stimuli of the innate or adaptive immune pathways. HPV accomplishes this by augmenting the expression of interferon-related developmental regulator 1 (IFRD1) in an EGFR-dependent manner. Restoration of NF κ B/RelA acetylation by IFRD1 shRNA, Cetuximab treatment or the HDAC1/3 inhibitor entinostat increases basal and induced cytokine expression. Similar observations are made in IFRD1-overexpressing HPV-induced cancer cells. Thus, our study reveals an EGFR-IFRD1 mediated viral immune evasion mechanism which can also be exploited by cancer cells.

INTRODUCTION

High-risk human papillomaviruses (hrHPVs) are absolutely species-specific small double-stranded DNA viruses that primarily target undifferentiated keratinocytes (KCs) of squamous epithelia via micro-wounds and abrasions. HrHPV infections can last up to two years despite viral activity in infected KCs, the expression of viral antigens and the presence of KC-expressed pattern recognition receptors (PRR)¹⁻⁴ that should lead to activation of innate and adaptive immune responses. This indicates that hrHPV has evolved mechanisms to transiently evade innate and adaptive immune mechanisms. Ultimately, the majority of hrHPV infections are controlled by the immune system, in particular by type 1 (IFN γ and TNF α) cytokine producing T cells⁵. In case of immune failure, hrHPV causes cancer of the anogenital and/or head and neck regions⁶.

Upon infection, hrHPV alters the immune-related response of keratinocytes to various innate and adaptive immune stimuli resulting in impaired expression of interferon (IFN)-stimulated genes (ISG), interferon regulatory transcription factor (IRF)-induced genes, and NFκB-induced genes^{3,7-12}, suggesting that HPV hampers STAT1 and NFκB activation. HPV-infected KCs display downregulated basal expression of *STAT1* and lowered STAT1 protein levels explaining the impaired expression of ISGs¹³⁻¹⁶. Furthermore, soon after infection HPV upregulates the cellular deubiquitinase ubiquitin carboxy-terminal hydrolase L1 (UCHL1) to impair PRR-induced NFκB activation by upstream interference with TRAF3, TRAF6 and NEMO⁸. The upregulation of UCHL1 however can not explain how the virus manages to suppress the KCs response to adaptive immune signals¹². In addition, repressing UCHL1 does not fully restore NFκB signaling via PRR⁸, suggesting that one or more additional mechanisms are in play to suppress NFκB signaling.

In this study, we analyze NFκB activation and subsequent cytokine/chemokine production following IFN γ and TNF α stimulation in uninfected and HPV-infected primary KCs. Our study reveals that RelA-acetylation, needed for NFκB transcriptional activity¹⁷, is impaired in hrHPV-infected KCs. The HPV-induced overexpression of the cellular protein interferon-related developmental regulator 1 (IFRD1) is shown to be instrumental in this process and involves

HDAC1 and/or 3. The augmented expression of IFRD1 is the result of the HPV-mediated upregulation of EGFR. Blocking of IFRD1 protein expression by shRNA or via the anti-EGFR antibody Cetuximab restores NFκB/RelA-mediated cytokine expression. Additional data suggest that IFRD1 may have a similar role in suppressing cytokine/chemokine production in HPV-positive cervical cancer cells.

RESULTS

HrHPV impairs the KCs cytokine response to IFN γ and TNF α

To evaluate if the KCs immune response following the exposure to IFN γ and/or TNF α is attenuated by hrHPV, we utilized a system that resembles the natural infection with hrHPV as closely as possible. Primary KCs stably maintaining the hrHPV genome as episomes (hrHPV+ KCs) display similar growth properties as non-transfected KC, and upon culture in organotypic raft cultures, mimic HPV infection *in vivo* as documented by genome amplification, late gene expression, and virus production during the differentiation dependent life cycle of HPV¹⁸⁻²⁰.

The presence of HPV type 16 (HPV16) was clearly associated with an impaired capacity to respond to IFN γ and to TNF α as shown by the lower mRNA expression and production of the IFN γ and/or TNF α -induced pro-inflammatory cytokines CCL2, RANTES (CCL5), IL8 and the chemokines CXCL9, 10 and 11 by KCs (Figure 1AB). Not only did the presence of HPV16 impair the production of cytokines, also the migration of peripheral blood mononuclear cells (PBMCs) to supernatants of IFN γ and TNF α -stimulated HPV16+ KCs was greatly impaired (Figure 1C).

These data suggest that hrHPV, besides impairing the innate immune response of KCs⁸, also suppresses the KCs response to the adaptive immune signals provided by IFN γ and TNF α .

The hrHPV-mediated deregulated expression of STAT1¹³⁻¹⁶ may explain the impaired cytokine expression by hrHPV-positive KCs upon IFN γ stimulation but not the impaired response to TNF α (IL8) or to IFN γ and TNF α (RANTES). Previously, we showed that hrHPV hampers phosphorylation of the NFκB subunit RelA (p65) upon stimulation with the innate pattern recognition receptor (PRR) ligand Poly(I:C)⁸. As TNF α stimulation rapidly induces the phosphorylation of RelA¹⁷, we tested whether hrHPV also hampers rapid TNF α -induced RelA phosphorylation by stimulating KCs and HPV16+ KCs for 0, 5, 15 or 30 minutes with TNF α . Western blotting showed that RelA was rapidly phosphorylated similarly in KCs and HPV16+ KCs, peaking after 15 minutes of TNF α stimulation (Figure 1D), indicating that the impairment of TNF α -induced responses seen in HPV16+ KCs was not due to altered RelA phosphorylation

after short-term TNF α stimulation. Activated NF κ B translocates to the nucleus where it is modified to regulate its DNA binding ability and transcriptional activity. Acetylation of the RelA subunit at lysine 310 (K310) is crucial in this process¹⁷. Strikingly, acetylated RelA K310 protein levels were lower in the HPV16+ KCs than in uninfected KCs, both in the absence of stimulation and after short-term TNF α stimulation (Figure 1D). The lowered basal RelA K310 acetylation state was verified in three independent primary KC and two independent HPV16+ KC cultures (Figure 1E), indicating that HPV hampers the activity of NF κ B already at steady-state levels. This was also reflected in a lowered basal cytokine gene expression in unstimulated HPV16+ KCs (Figure 1F).

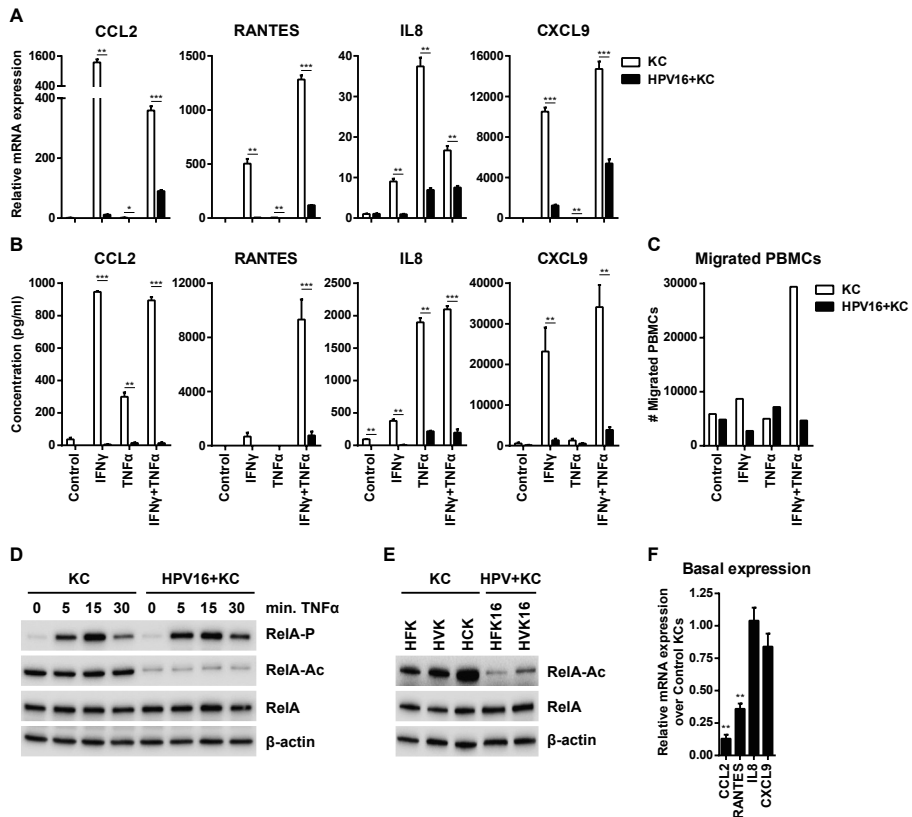


Figure 1: HPV16 impairs IFN γ and TNF α -induced cytokine production and RelA K310 acetylation in KCs

(A) RT-qPCR of CCL2, RANTES, IL8 and CXCL9 expression by 24 hours control, IFN γ and/or TNF α -stimulated undifferentiated KCs or HPV16+ KCs. Gene expression was normalized using GAPDH as the calibrator gene. Fold changes over control-stimulated undifferentiated KCs were calculated and depicted.

(B) ELISA for CCL2, RANTES, IL8 and CXCL9 in cleared supernatants of 24 hours control, IFN γ and/or TNF α -stimulated undifferentiated KCs or HPV16+ KCs.

(C) PBMCs migration towards cleared supernatants of 24 hours control, IFN γ and/or TNF α -stimulated KCs or HPV16+ KCs. A representative example of 3 different donors is shown.

(D) RelA phosphorylation, acetylation and total levels in KCs and HPV16+ KCs stimulated with TNF α for 0, 5, 15 and 30 minutes.

(E) RelA acetylation and total levels at steady-state in three human primary keratinocyte (KC) donor pools originating from human foreskin keratinocytes (HFK), human vaginal keratinocytes (HVK) or human cervical keratinocytes (HCK) and two HPV16+ genome transfected primary KC pools foreskin (HFK16) or vaginal (HVK16) origin.

(F) RT-qPCR of CCL2, RANTES, IL8 and CXCL9 in HPV16+ KCs and KCs. Gene expression was normalized using GAPDH as the calibrator gene. Gene expression in HPV16+ KCs was standardized over KCs.

All data are representative for at least three independent experiments. Error bars indicate SD. P-values were determined via Welch-corrected unpaired t tests. * $p < 0.05$, ** $p < 0.01$, *** $p < 0.001$.

HrHPV upregulates IFRD1 to impair RelA K310 acetylation

Acetylation of RelA K310 can be regulated by the lysine acetyl transferases (KAT) PCAF (KAT2B), CBP (KAT3A), p300 (KAT3B), and TIP60 (KAT5) as well as the histone deacetylases (HDAC) 1 and 3¹⁷. Since our results imply that hrHPV has a mechanism either to deacetylate or impair the acetylation of RelA, we screened our validated micro array data¹² for genes involved in regulating RelA K310 acetylation. High-risk HPV did not significantly influence *histone deacetylase (HDAC1 to 11)* or *sirtuin (SIRT1 to 7)* expression (Figure 2A). The only significantly upregulated gene was the lysine acetyl transferase *CREBBP (KAT3A)*, confirming previous observations stating that HPV upregulates CREBBP to enhance expression from episomal DNA^{21,22}. However, as CREBBP acetylates RelA its upregulation can not explain the observed lower levels of RelA K310 acetylation in hrHPV-infected KCs under steady state conditions. Interestingly, the micro array data also showed the upregulation of Interferon-related developmental regulator 1 (*IFRD1*) (Figure 2B), which previously was shown to complex HDAC1²³ and HDAC3 to RelA causing its deacetylation at lysine 310 in the mouse myoblast cell line C2C12²⁴. We hypothesized that it may fulfill a similar role in human KCs. Therefore, RT-qPCR and western blotting was used to confirm that *IFRD1* gene expression (Figure 2C left) and IFRD1 protein levels (Figure 2D left) were elevated in two independent HPV16+ KC cultures. Knock-down of the polycistronic mRNA of HPV16 by a

siRNA against HPV16 E2 in HPV16+ KCs resulted in the reduction of HPV16 *E1*, *E2*, *E6* and *E7* expression (Supplementary Fig. S1), *IFRD1* mRNA (Figure 2C middle) and IFRD1 protein levels (Figure 2D middle), indicating that the augmented IFRD1 levels in hrHPV+ KCs are the result of the presence of hrHPV. Reciprocally, when undifferentiated KCs were infected with native HPV16 virions, *IFRD1* mRNA (Figure 2C right) and IFRD1 protein (Figure 2D right) levels were clearly enhanced after 2 days of infection. Furthermore, immunohistochemistry of HPV-positive vulvar lesions revealed the presence of IFRD1 in the nuclei of cells positive for HPV16 E2 (reflecting HPV-infected cells)²⁵, but not in the nuclei of already transformed KCs (identified through p16 staining^{25,26} or undifferentiated (E2 and p16 negative) healthy tissue (Figure 2E).

We then asked if the hrHPV-induced increased levels of IFRD1 affected RelA K310 acetylation also in human undifferentiated KCs. Indeed, when lentivirus-delivered siRNA against *IFRD1* was used to lower IFRD1 protein expression a concomitant increase in the steady-state levels of acetylated RelA K310 in HPV16+ KCs was seen when compared to control knock-down HPV16+ KCs (Figure 2F; Supplementary Fig. S2A). Furthermore, a small increase in total RelA protein levels was observed. The gain in acetylated RelA K310 translated into a higher basal expression and secretion of cytokines in IFRD1 KD cells (Figure 2GHI), indicating that IFRD1 is involved in the deregulation of steady-state inflammatory gene expression levels in HPV16+ KCs. The dampening effect of *IFRD1* on the NF κ B-regulated cytokine expression became even more apparent when the KCs were stimulated with both IFN γ and TNF α (Figure 2HI). The cytokine levels produced after stimulation were much higher in IFRD1 KD HPV16+ KCs than in control KD HPV16+ KCs. Moreover, *IFRD1* knock-down augmented the ability of HPV16+ KCs to attract PBMCs (Figure 2J). The main results were recapitulated in HPV18-infected KCs (Supplementary Fig. S3), suggesting that IFRD1 may form a general mechanism exploited by any hrHPV type.

As the effect of IFRD1 occurred directly at the level of RelA, the influence of IFRD1 on the response of HPV16+ KCs to Poly(I:C) stimulation, previously shown by us to be impaired in hrHPV-infected KCs⁸, was also tested. Knock-down of *IFRD1* resulted in an enhanced expression of *CCL2*, *RANTES*, *IL8*

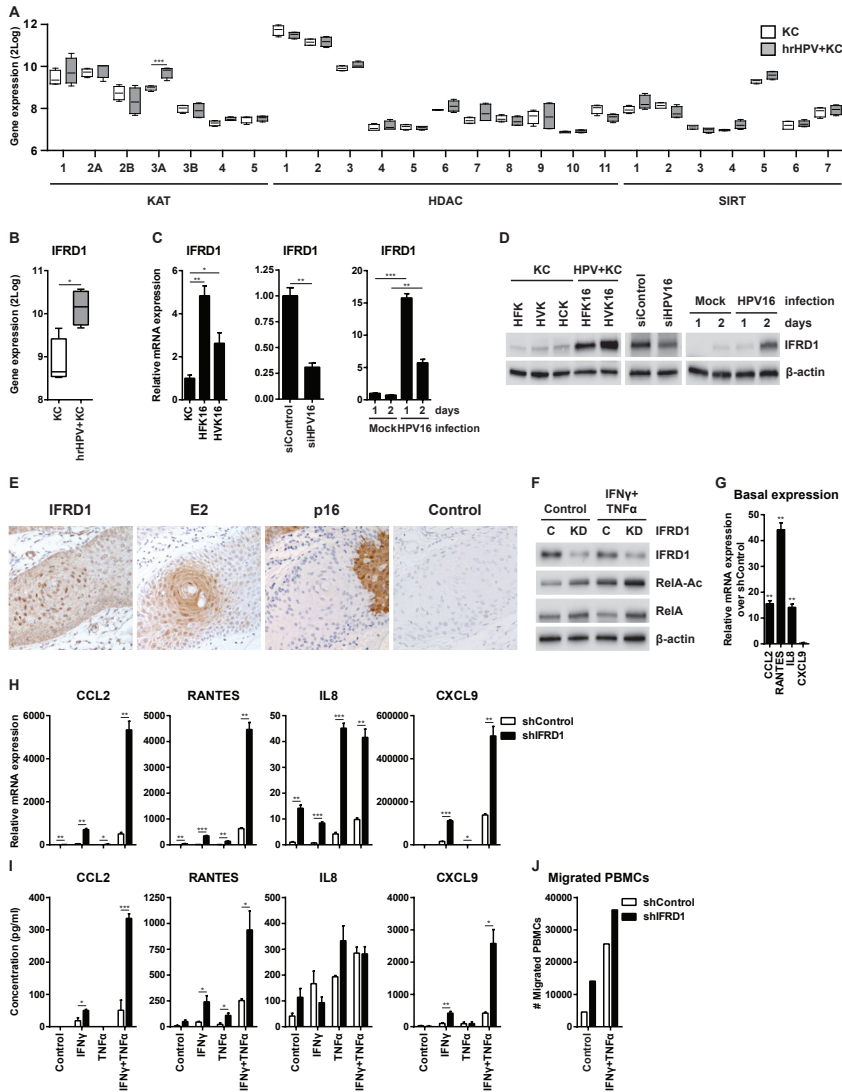


Figure 2: HrHPV upregulates IFRD1 to impair RelA K310 acetylation and basal cytokine expression

Microarray intensities for (A) all KATs, HDACs and SIRT1-7, and (B) IFRD1 in 4 independent KCs and 4 independent hrHPV+ KCs represented in a box plot. The box contains the 1st quartile up to the 3rd quartile, the median is represented as a line, whiskers represent the values of the outer 2 quartiles.

(C) *IFRD1* mRNA expression of one representative control primary KC culture and two HPV16+ KC culture (left panel), in HFK16 cells transfected with siControl or siHPV16 (middle panel) and in primary KCs that are either mock infected or infected with native HPV16 virions (right panel), as measured by RT-qPCR.

(D) *IFRD1* protein expression in three human primary keratinocyte (KC) donor pools originating from human foreskin keratinocytes (HFK), human vaginal keratinocytes (HVK) or human cervical keratinocytes (HCK) and two HPV16+ genome transfected primary KC pools foreskin (HFK16) or vaginal (HVK16) origin (left panel) in HFK16 cells transfected with siControl or siHPV16 (middle panel) and in primary KCs that are either mock infected or infected with native HPV16 virions (right panel), as measured by western blot.

(E) Immunohistochemical staining for *IFRD1*, HPV16 E2, p16 and negative antibody control of a vulvar intraepithelial neoplasia (VIN) lesion, one representative donor of two shown. Counterstaining was done using hematoxylin. Arrows indicate sites where E2 and nuclear *IFRD1* are expressed. Scale bar 500 μ m.

(F) *IFRD1*, RelA K310 acetylation and total RelA levels in 24 hours non- or IFN γ and TNF α -stimulated control or *IFRD1* knock-down (KD) HPV16+ KCs.

(G) RT-qPCR of *CCL2*, *RANTES*, *IL8* and *CXCL9* expression in steady-state control or *IFRD1* KD HPV16+ KCs.

(H) RT-qPCR of *CCL2*, *RANTES*, *IL8* and *CXCL9* expression in 24 hours non- or IFN γ and/or TNF α -stimulated control or *IFRD1* KD HPV16+ KCs.

(I) ELISA for *CCL2*, *RANTES*, *IL8* and *CXCL9* in cleared supernatants of 24 hours non- or IFN γ and/or TNF α -stimulated control or *IFRD1* KD HPV16+ KCs.

(J) PBMCs migration towards cleared supernatants of 24 hours non- or IFN γ and TNF α -stimulated control or *IFRD1* KD HPV16+ KCs. A representative example of 3 different donors is shown.

These data are representative for at least three independent experiments. Error bars indicate SD. P-values were determined via Welch-corrected unpaired t tests. * $p < 0.05$, ** $p < 0.01$, *** $p < 0.001$.

and *CXCL9* following PRR stimulation with Poly(I:C) (Supplementary Fig. S4).

Thus, hrHPV upregulates the expression of *IFRD1* soon after infection, thereby effectively decreasing the basal levels of transcriptionally active RelA and as a consequence the levels of pro-inflammatory cytokines induced via various innate and adaptive immune-mediated NF κ B stimulatory pathways.

EGFR-signaling mediates the increased expression of *IFRD1*

Growth factors, such as NGF, FGF or EGF, have previously been shown to induce the expression of *Tis* family genes, which also includes *IFRD1*, in rat neocortical astrocytes and chromaffin cell line PC12, mouse C243 and IEC-18, and mammary epithelial cells²⁷. The hrHPV E5 protein is known to affect different aspects of EGF receptor (EGFR) signaling and expression²⁸. Verification of EGFR expression in our model showed that *EGFR* mRNA expression (Figure 3A) and membrane-bound protein expression (Figure 3B) were higher in hrHPV+ KCs than in non-infected KCs. When we transfected cDNA for E2 (as

control), E5 or a mix of several other HPV proteins, only E5 enhanced *EGFR* expression (Figure 3C). To test if EGFR signaling had a similar effect on IFRD1 in human primary KCs, the clinically used anti-EGFR antibody Cetuximab was employed to block EGFR signaling. Indeed, *IFRD1* expression decreased in HPV16+ KCs, but not in uninfected KCs, when treated with Cetuximab (Figure 3D). IFRD1 protein levels also decreased dose-dependently in both Cetuximab-treated non-infected KCs and HPV16+ KCs (Figure 3E). Notably, the isotype control antibody Rituximab (anti-CD20) had no effect (Figure 3DE). Thus EGFR signaling does not only induce *IFRD1* gene expression but also stabilizes IFRD1 protein levels. Relative density analysis revealed that in Cetuximab-treated HPV16+ KCs the protein levels of IFRD1 decreased while concomitantly the levels of RelA K310 acetylation increased in a dose-dependent fashion. Total RelA levels were unaffected (Figure 3F). These results indicated that the HPV-induced expression of IFRD1 is mediated via the EGFR signaling pathway and implied that Cetuximab treatment may enhance the hrHPV+ KCs pro-inflammatory cytokine response to immune stimuli. Indeed, upon IFN γ and TNF α stimulation Cetuximab-treated HPV16+ KCs expressed higher levels of indicated cytokine genes than Rituximab-treated cells (Figure 3G) as well as higher levels of secreted cytokines (Figure 3H). In uninfected KCs treatment with Cetuximab decreased the already low levels of IFRD1 protein, and although this led to increased cytokine gene expression after IFN γ and TNF α -stimulation no additional increase in the already high levels of secreted cytokines was observed (Figure 3GH). The absence of cytokine production in Cetuximab-treated HPV16+ KC and uninfected KCs that were not stimulated with IFN γ and TNF α shows that binding of Cetuximab to EGFR *per se* does not result in the stimulation of cytokine production (Figure 3GH).

As EGFR signaling involves the downstream partners PI3K, mTOR, MEK1, RAF and JNK, we selectively inhibited these proteins using small molecule inhibitors in HPV16+ KCs and observed that selective inhibition of mTOR (Rapamycin), MEK1 (PD98059) and RAF (GW5074) but not PI3K (LY94002) or JNK (SP60025) resulted in decreased expression of IFRD1 (Figure 3I). Thus EGFR-mediated upregulation of IFRD1 is fundamental to the impaired NFκB-induced cytokine response of hrHPV-infected KCs to innate and adaptive immune stimuli.

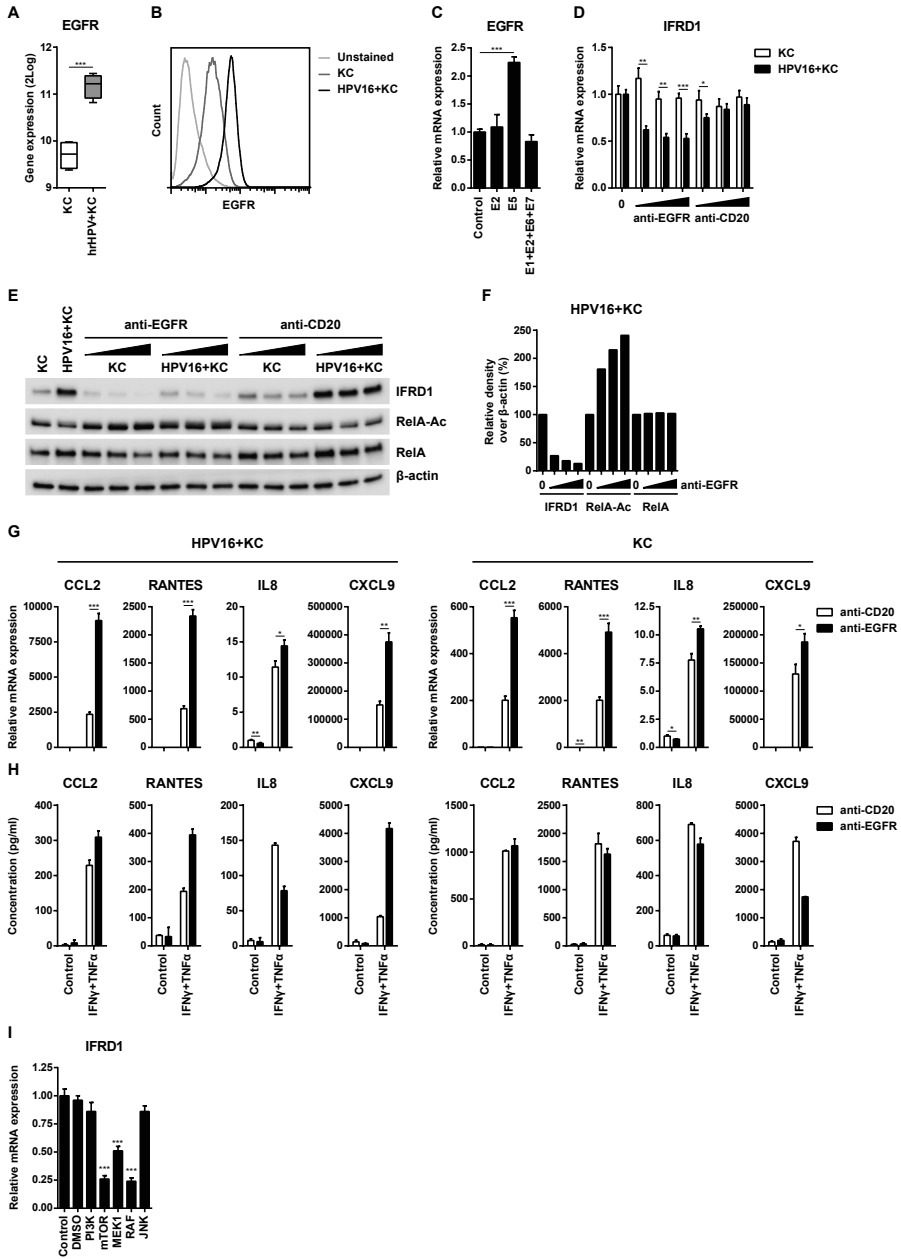


Figure 3: Blocking EGFR-signaling decreases IFRD1 levels and rescues cytokine production by hrHPV+ KCs

(A) Microarray intensities for EGFR in KCs (n=4) and hrHPV+ KCs (n=4) represented in a box plot.
 (B) Histogram of EGFR surface protein expression on KCs and HPV16+ KCs as determined by flow cytometry.
 (C) RT-qPCR of EGFR expression in KCs transfected with cDNA for E2, E5, E1+E2+E6+E7, or empty control.
 (D) RT-qPCR of IFRD1 expression in KCs and HPV16+ KCs treated for 72 hours with 0, 0.1, 1 or 10 $\mu\text{g ml}^{-1}$ anti-EGFR or anti-CD20.
 (E) IFRD1, RelA K310 acetylation and total RelA levels in KCs and HPV16+ KCs treated for 72 hours with 0, 0.1, 1 or 10 $\mu\text{g ml}^{-1}$ anti-EGFR or anti-CD20.
 (F) Quantified protein levels of IFRD1, RelA K310 acetylation, and RelA over β -Actin in HPV16+ KCs treated for 72 hours with 0, 0.1, 1 or 10 $\mu\text{g ml}^{-1}$ anti-EGFR (western blot 2D). The expression levels of the 0 $\mu\text{g/ml}$ treated HPV+ KCs were set as 100%.
 (G) RT-qPCR of CCL2, RANTES, IL8 and CXCL9 expression in 24 hours non- or IFN γ and TNF α -stimulated, anti-CD20 or anti-EGFR-treated HPV16+ KCs (left) and KCs (right).
 (H) ELISA for CCL2, RANTES, IL8 and CXCL9 in cleared supernatants of 24 hours non- or IFN γ and TNF α -stimulated, anti-CD20 or anti-EGFR-treated HPV16+ KCs (left) and KCs (right).
 (I) RT-qPCR of IFRD1 expression in HPV16+ KCs treated with inhibitors of PI3K (LY94002, 25 μM), mTOR (Rapamycin, 50 nM), MEK1 (PD98059, 50 μM), RAF (GW5074, 20 μM), and JNK (SP60025, 20 μM). Gene expression was normalized using GAPDH as the calibrator gene. Fold changes over Control were calculated and depicted.
 These data are representative for at least three independent experiments, except for figure H which was performed once. Error bars indicate SD. P-values were determined via Welch-corrected unpaired t tests. * $p < 0.05$, ** $p < 0.01$, *** $p < 0.001$.

HDAC1/3 inhibition stimulates cytokine production

IFRD1-mediated RelA deacetylation required the recruitment of HDAC1 and/or 3 to the RelA-IFRD1 complex in the mouse myoblast cell line C2C12²⁴. To test if these HDACs played a similar role in human hrHPV+ KCs, the effect of HDAC inhibition was tested in HPV16+ KCs and non-infected KCs. A dose-titration of the HDAC1/3-specific inhibitor entinostat (MS-275), and the prototypic pan-HDAC inhibitors trichostatin A (TSA), sodium butyrate (NaBu) and the FDA-approved vorinostat (SAHA) was performed to study RelA K310 acetylation. All pan-HDAC inhibitors increased RelA acetylation in KCs at the lowest concentration used (Figure 4A & Supplementary Fig. S2B) but at higher doses cells suffered from toxic effects as observed by microscopy. However, HPV16+ KCs did survive entinostat treatment, and clearly this HDAC1/3 inhibitor increased RelA K310 acetylation in HPV16+ KCs (Figure 4A & Supplementary Fig. S2B). This indicated that HDAC1 and/or 3 are indeed specifically involved in the deacetylation of RelA in hrHPV+ KCs. Entinostat treatment of HPV16+ KCs not only restored RelA K310 acetylation but also released the suppressive effect of IFRD1 on cytokine production. Treated HPV16+ KCs displayed a

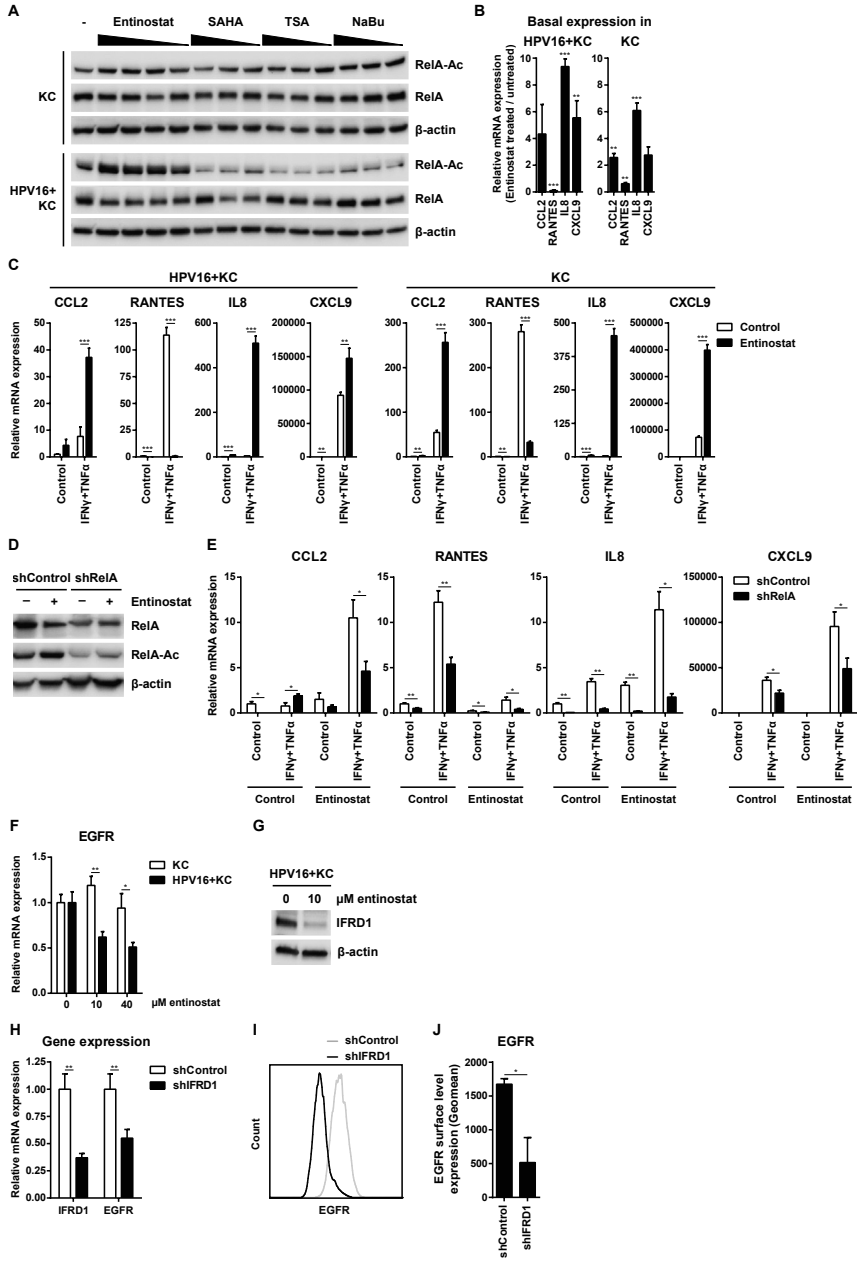


Figure 4: Entinostat treatment reveals involvement of HDAC1/3 in RelA deacetylation in HPV16+ KCs

(A) RelA K310 acetylation and total RelA levels in KCs and HPV16+ KCs treated with decreasing doses of entinostat (40, 20, 10 and 2 μM), SAHA (10, 5 and 1 μM), TSA (5, 1 and 0.333 μM) or NaBu (10, 5 and 1 mM).

RT-qPCR of CCL2, RANTES, IL8 and CXCL9 expression in steady-state (B) or 24 hours non- or IFNγ and TNFα-stimulated (C) control or entinostat (10 μM) pre-treated HPV16+ KCs.

(D) Total RelA levels and RelA K310 acetylation non- or entinostat-treated control or RelA knock-down (KD) HPV16+ KCs.

(E) RT-qPCR of CCL2, RANTES, IL8 and CXCL9 expression in 24 hours non- or IFNγ and TNFα-stimulated non- or entinostat-treated control or RelA knock-down (KD) HPV16+ KCs.

(F) RT-qPCR of EGFR expression in KCs and HPV16+ KCs treated with increasing doses of entinostat (0, 10 or 40 μM). Gene expression was normalized using GAPDH as the calibrator gene.

(G) IFRD1 in control or entinostat (10 μM) pre-treated HPV16+ KCs.

(H) RT-qPCR of IFRD1 and EGFR expression in control or IFRD1 KD HPV16+ KCs. Gene expression was normalized using GAPDH as the calibrator gene.

Histogram (I) and Geo mean (J) of EGFR expression on control or IFRD1 KD HPV16+ KCs as determined by flow cytometry. SEM of two independent experiments.

These data are representative for at least two independent experiments. Error bars indicate SD. P-values were determined via Welch-corrected unpaired t tests. * $p < 0.05$, ** $p < 0.01$, *** $p < 0.001$.

higher basal expression for 3 out of 4 tested cytokines when compared to their untreated counterparts (Figure 4B). Moreover, when stimulated with IFNγ and TNFα both KCs and HPV16+ KCs displayed a higher expression of CCL2, IL8 and CXCL9, although the expression of RANTES was abrogated (Figure 4C). To confirm the involvement of RelA in this process, RelA was knocked-down in HPV+ KCs (Figure 4D), after which the cells were treated with entinostat and stimulated with IFNγ and TNFα. Indeed, RelA acetylation and cytokine production was increased in the control knock-down cells after stimulation with IFNγ and TNFα when treated with entinostat (Figure 4DE). However, when RelA was knocked-down in HPV16+ KCs, the cytokine expression was abrogated despite treatment with entinostat (Figure 4E).

Previously, it was shown that HDAC inhibition abrogates EGFR expression^{29,30}, indicating that EGFR expression is dependent on acetylation events. Indeed, entinostat treatment dose-dependently abrogated EGFR expression in hrHPV+ KCs, but did not influence the expression in KCs (Figure 4F). Furthermore, entinostat treatment resulted in a reduced level of IFRD1 protein in hrHPV+ KCs (Figure 4G), which made us wonder if IFRD1 could regulate EGFR expression. Therefore, IFRD1 was knocked-down in hrHPV+ KCs and this resulted in lower EGFR expression (Figure 4H) and a lower level

of membrane-bound EGFR than control-treated hrHPV+ KCs (Figure 4IJ), indicating that IFRD1 can control *EGFR* expression.

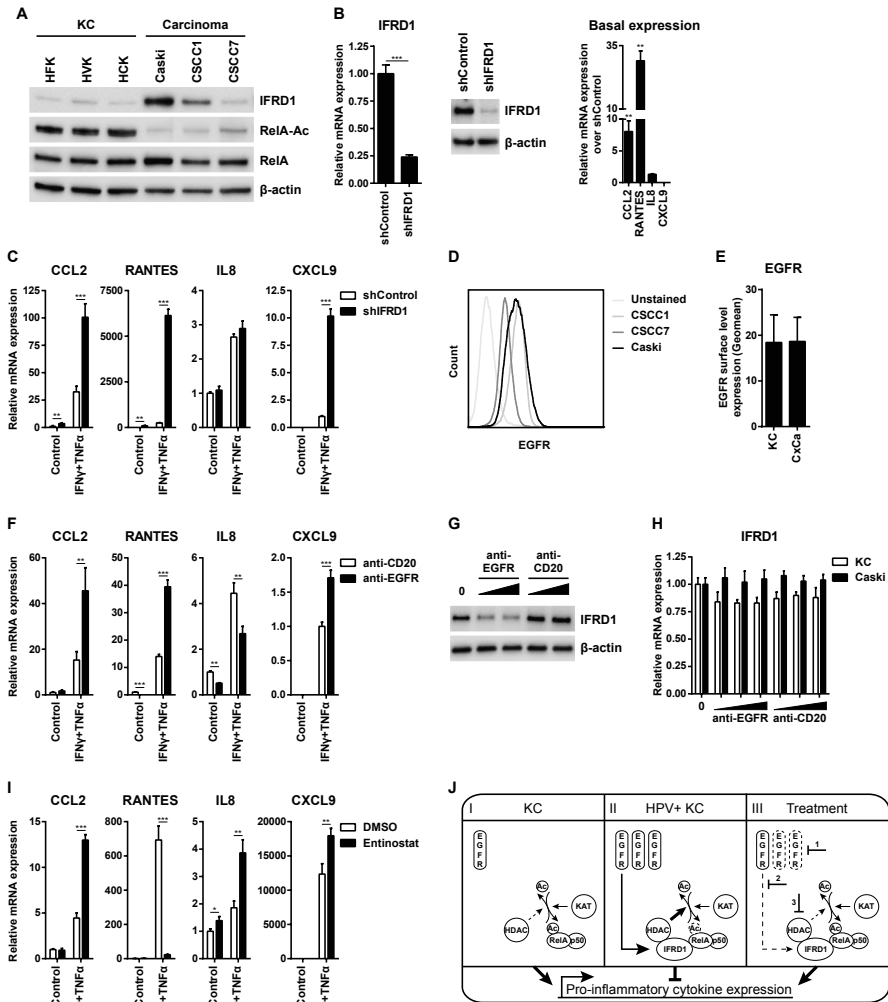


Figure 5: Role of IFRD1 in hrHPV+ cervical cancer cells

(A) *IFRD1*, *RelA* acetylation and total *RelA* levels at steady-state in three KC donors and three HPV16-induced CxCa lines.

(B) RT-qPCR of *IFRD1*, *CCL2*, *RANTES*, *IL8* and *CXCL9* expression and *IFRD1* protein levels in

steady-state control or IFRD1 KD Caski cells.

(C) RT-qPCR of IFRD1, CCL2, RANTES, IL8 and CXCL9 expression in 24 hours non- or IFN γ and TNF α -stimulated control or IFRD1 KD Caski cells.

(D) Histogram of EGFR expression on three HPV16-induced CxCa lines.

(E) Geo mean of EGFR expression on KCs and CxCa as determined by flow cytometry. SEM of two independent experiments.

(F) RT-qPCR of CCL2, RANTES, IL8 and CXCL9 expression in 24 hours non- or IFN γ and TNF α -stimulated anti-CD20 or anti-EGFR-treated Caski cells.

(G) IFRD1 and RelA K310 acetylation status in Caski cells treated for 72 hours with 0, 1 or 10 $\mu\text{g ml}^{-1}$ anti-EGFR (Cetuximab) or anti-CD20 (Rituximab).

(H) RT-qPCR of IFRD1 expression in KCs and Caski cells treated for 72 hours with 0, 0.1, 1 or 10 $\mu\text{g ml}^{-1}$ anti-EGFR or anti-CD20.

(I) RT-qPCR of CCL2, RANTES, IL8 and CXCL9 expression in 24 hours non- or IFN γ and TNF α -stimulated control (DMSO) or entinostat-treated Caski cells.

(J) Schematic representation of IFRD1-mediated RelA (de-)acetylation. I) In KCs, RelA acetylation is positively regulated by KATs, resulting in the production of pro-inflammatory cytokines. HDACs may suppress this process. II) In HPV+ KCs, elevated EGFR levels can induce the expression of IFRD1, which can mediate RelA deacetylation by forming a bridge between RelA and HDAC1 and/or 3, hampering pro-inflammatory gene expression. III) Interfering with EGFR signaling (1 and 2) or HDAC function (3) may lower IFRD1 levels, restoring the RelA acetylation balance, augmenting pro-inflammatory gene expression.

Error bars indicate SD. P-values were determined via Welch-corrected unpaired t tests. * $p < 0.05$, ** $p < 0.01$, *** $p < 0.001$.

IFRD1 hampers the response of cancer cells to IFN γ and TNF α

To evaluate if an increased expression of IFRD1 could also play a role in HPV16-induced squamous cell carcinoma, we analyzed the cell line Caski, as well as the two early passage cervical cancer cell lines, C5CC1 and C5CC7³¹. IFRD1 protein expression differed between the cell lines (Figure 5A), but was increased in Caski and C5CC1 when compared to normal KCs. RelA K310 acetylation was lower in all three cervical cancer cell lines than in uninfected KCs (Figure 5A & Supplementary Fig. S2C). For the Caski and C5CC1 lines this may be explained by the presence of upregulated IFRD1. However, the lack of RelA K310 acetylation in the C5CC7 line indicates that besides IFRD1 also other mechanisms can alter the acetylation of RelA K310 in these squamous cancer cells.

Because IFRD1 was upregulated in the Caski and C5CC1 cells we studied the effects of IFRD1 using these cell lines. IFRD1 knock-down in the C5CC1 cells did not alter basal cytokine expression levels (Supplementary Fig. S5A), but IFRD1 knock-down in the Caski cells resulted in a direct increase of the basal expression levels of CCL2 and RANTES (Figure 5B). Furthermore, both cell lines showed increased cytokine gene levels upon IFN γ and TNF α stimulation

when IFRD1 was knocked-down as compared to their control knock-down counterparts (Figure 5C and Supplementary Fig. S5B).

CSCC1 and Caski cells express EGFR (Figure 5D) at a level that is similar to that of uninfected KCs (Figure 5E). However the downstream signaling pathway is known to be constitutively higher in HPV-induced cancer cells³². As a consequence, the treatment of Caski and CSCC1 cancer cells with the anti-EGFR antibody Cetuximab resulted in a higher production of IFN γ and TNF α -induced cytokines than when the cancer cells were treated with the control anti-CD20 antibody Rituximab (Figure 5F and Supplementary Fig. S5C). The enhanced response to IFN γ and TNF α was associated with a concomitant decrease in IFRD1 protein levels (Figure 5G), but not mRNA expression (Figure 5H), upon EGFR blockade. Similarly, treatment of Caski and CSCC1 cancer cells with entinostat resulted in a higher production of *CCL2*, *IL8* and *CXCL9* by the cancer cells when stimulated with IFN γ and TNF α than DMSO carrier control treated cells (Figure 5I and Supplementary Fig. S5D). Congruent with our earlier observations, *RANTES* levels diminished after entinostat treatment. These results suggest that IFRD1 may also play a role in suppressing the response of cancer cells to immune stimuli such as IFN γ and TNF α .

DISCUSSION

Using a unique *in vitro* model we here show that hrHPV infection leads to the upregulated expression of endogenous IFRD1 to deregulate the K310 acetylation of NFκB/RelA. As a result hrHPV-infected KCs display an impaired production of pro-inflammatory cytokines and chemokines, and a reduced capacity to attract immune cells. The increased expression of IFRD1 in hrHPV+ KCs is mediated by EGFR signaling via mTOR, RAF and/or MEK1. Knock-down of *IFRD1* with siRNA or indirectly via blockade of EGFR with the clinically used EGFR-specific antibody Cetuximab, resulted in decreased IFRD1 mRNA and protein levels, increased NFκB/RelA K310 acetylation and enhanced expression and production of pro-inflammatory cytokines and chemokines by hrHPV+ KCs. The use of entinostat indicated that HDAC1 and/or 3 are involved in lowering K310 acetylation of NFκB/RelA. These conclusions are schematically represented in figure 5J.

EGFR activation on epithelial cells has been shown to result in a decreased production of CCL2, RANTES and CXCL10 and increased production of IL8. Inhibition of EGFR signaling with blocking antibodies or tyrosine kinase inhibitors can reverse the effect on these cytokines as well as result in an increased epithelial immune infiltrate *in vivo*³³⁻³⁵. Interestingly, virus-induced EGFR-activation has been implicated as novel mechanism for respiratory viruses to suppress antiviral host responses³³. The exact underlying mechanism on EGFR-mediated immune suppression remained unclear, albeit that ERK1/2 signaling was shown to be involved in regulating cytokine production and skin inflammation³⁶. Using the EGFR blocking antibody Cetuximab in the absence of an additional EGFR stimulus such as TGFα we found similar effects on the cytokine production of HPV16+ KCs. In KCs the expression of EGFR and IFRD1 are tightly linked as EGFR inhibition reduced the expression and protein levels of IFRD1, via mTOR, RAF and/or MEK1, but not PI3K or JNK. This fits with the involvement of ERK1/2 in regulating cytokine production (Pastore et al., 2005) since RAF and MEK1 are just upstream of these kinases. Based on our data, the previously observed EGFR activation-induced suppression of cytokine production and immune cell infiltration of epithelia can be explained by upregulation of IFRD1 and subsequent suppression of NFκB signaling. Our

data suggest that EGFR-driven overexpression of IFRD1 may also play a role in deregulating NF κ B-signaling in HPV-induced tumor cells. Knock-down of IFRD1 results in an increased production of pro-inflammatory cytokines and chemokines by tumor cells when stimulated with IFN γ and TNF α . Furthermore, blocking of the EGFR by Cetuximab resulted in a decrease of IFRD1 protein levels as well as increased cytokine production. The HPV oncoproteins are also known to directly intervene with NF κ B signaling. Studies with transfected or transformed cells – resembling protein expression in tumor cells – show that E6 and/or E7 proteins inhibit basal and TNF α -inducible NF κ B activity³⁷ by influencing NF κ B localization^{38,39} and activation⁴⁰⁻⁴³.

Studies in immunosuppressed patients and healthy individuals show a key role for the adaptive immune response, in particular that of a strong type 1 (IFN γ and TNF α)-associated HPV early antigen-specific T cells in the protection against progressive disease⁵. This notion is sustained by the clinical responses of patients treated with HPV-specific therapeutic vaccines⁵. Ample reasons, therefore, for HPV to also develop strategies preventing KCs to respond to these cytokines. Our data shows that HPV deploys multiple strategies to interfere with induced RelA-associated NF κ B signaling. HPV utilizes the cellular deubiquitinase UCHL1 to interfere with TRAF3, TRAF6 and NEMO function⁸ and here we show that HPV also upregulates the expression of endogenous IFRD1 to deregulate the K310 acetylation of NF κ B. Furthermore, the E7 protein of hrHPV has been shown to bind HDAC1 and prevent acetylation of histones, thereby suppressing TLR9 signaling⁴⁴, but E7 can also displace HDACs resulting in enhanced hypoxia-inducible factor 1 α transcriptional activity⁴⁵. It is not unusual for viruses to target NF κ B activation^{46,47}, and hampering RelA acetylation is a common strategy. For instance, the N-terminus of the orf virus (ORFV) protein 002 inhibits acetylation of RelA by blocking phosphorylation of RelA S276 and subsequent recruitment of acetylases p300 and CBP⁴⁸, and the A238L protein of African swine fever virus (ASFV) hampers RelA K310 acetylation by inhibiting RelA-p300 interaction⁴⁹. We here postulate that hrHPV does not hamper KATs in acetylating RelA, but rather recruits a mediator to enhance HDAC-mediated RelA deacetylation. Together with our observation that HPV lowers basal cytokine expression in resting KCs due to the presence of IFRD1, we suggest that impairment of immune driven RelA-associated

NFκB-responsive gene expression is crucial for the virus to persist. This viral strategy has not been reported before, but as discussed above may also be employed by respiratory viruses that activate EGFR³³.

All together, our data indicate that HPV upregulates EGFR to drive IFRD1 expression as a tool to decrease basal and adaptive-immune system driven cytokine expression. This may allow hrHPV to evade the host's immune response. It is highly likely that this mechanism plays a role in other viral infections too and even extends to tumors.

METHODS

Ethics Statement

The use of discarded human foreskin, cervical and vaginal keratinocyte tissues to develop cell lines for these studies was approved by the Institutional Review Board at the Pennsylvania State University College of Medicine and by the Institutional Review Board at Pinnacle Health Hospitals. The Medical Ethical Committee of the Leiden University Medical Center approved the human tissue sections (healthy foreskin, healthy cervix, HPV16- or 18-positive cervical neoplasias) used for staining. All sections and cell lines were derived from discarded tissues and de-identified, therefore no informed consent was necessary.

Cell culture

Primary cultures of human epithelial keratinocytes (KCs) were established from foreskin, vaginal, vulva and cervical tissues as previously described³ and grown in keratinocyte serum-free medium (K-SFM; Medium 154 supplemented with HKGS kit, Invitrogen, Breda, The Netherlands). KCs stably maintaining the full episomal HPV genome following electroporation (HPV-positive KCs) were grown in monolayer culture using E medium in the presence of mitomycin C (Sigma-Aldrich) treated J2 3T3 feeder cells^{19,20} for two passages and were then adapted to K-SFM for one passage before experimentation. J2 3T3 mouse fibroblasts, Caski, CSCC1, CSCC7 and SiHa cell-lines were cultured in Iscove's modified Dulbecco's medium supplemented with 8% fetal bovine serum, 2 mM l-glutamine and 1% penicillin-streptomycin (complete IMDM medium) (Gibco-BRL, Invitrogen, Breda, The Netherlands).

HPV16 infection of non-infected keratinocytes

Primary basal layer human foreskin keratinocytes were seeded 75.000 cells per well to 24-wells plates and allowed to attach for 48 hours. Cells received fresh medium (Mock infected) or medium containing native HPV16 isolated from raft cultures at MOI 100 for 24 hours. Cells were washed and harvested for either RT-qPCR or western blotting analysis.

IFRD1 and RelA knock-down in HPV-positive KCs

shRNA's were obtained from the MISSION TRC-library of Sigma-Aldrich (Zwijndrecht, The Netherlands). The MISSION shRNA clones are sequence-verified shRNA lentiviral plasmids (pLKO.1-puro) provided as frozen bacterial glycerol stocks (Luria Broth, carbenicillin at 100 µg/ml and 10% glycerol) in *E. coli* for propagation and downstream purification of the shRNA clones. pLKO.1 contains the puromycin selection marker for transient or stable transfection. The construct against IFRD1 (NM_001550) was TRCN0000156194:

CCGGCAGTTCTGAAACAGTTTCTTTCTCGAGAAAGAACTGTTTCA-GAACTGTTTTT, RelA (NM_021975) was TRCN0000014687: CCGGCCT-GAGGCTATAACTCGCCTACTCGAGTAGGCGAGTTATAGCCTCAGTTTTT, and the control was: SHC004 (MISSION TRC2-pLKO puro TurboGFP shRNA Control vector): CCGGCGTGATCTTCACCGACAAGATCTCGAGATCTTGTCGGTGAAGATCACGTTTTT. HPV16-positive KCs at ~60% confluence were transduced with lentivirus at MOI 5-10 over night, after which medium was replaced. At least 72 hours post-transduction cells were stimulated as indicated and target gene expression was assayed by RT-qPCR or western blotting.

HPV knock-down in HPV-positive KCs

SilencerSelectsiRNAagainstHPV16E2(AACACUACACCCAUAGUACAUtt) was designed using siRNA Target Finder software (Ambion, Invitrogen). Blast search revealed that the designed E2 siRNA does not match with the known human transcriptome. E2 and Negative control #2 (NC2) siRNA (sequence not provided by manufacturer) were purchased from Ambion. HPV16+ KCs were transfected with 50 nM siRNA E2 or NC2 using Lipofectamine 2000 (Invitrogen) according to the manufacturer's instructions. 48 hours post-transfection cells were harvested or stimulated as indicated and target gene expression was assayed by RT-qPCR or western blotting.

Transfection of HPV genes into non-infected keratinocytes

Non-infected primary KCs were seeded 50.000 cells per well to 24-wells plates and allowed to attach over night. Cells were transfected with 500 ng DNA using Lipofectamine (Invitrogen), according to the manufacturer's instructions. Cells were maintained in E-medium. 72 hours post-transfection cells were harvested and target gene expression was assayed by RT-qPCR.

EGFR signaling blocking

Subconfluent cells were cultured in respective complete growth medium in presence of Cetuximab (0.1, 1 or 10 $\mu\text{g ml}^{-1}$; Merck serono), Rituximab (0.1, 1 or 10 $\mu\text{g ml}^{-1}$; Roche), rapamycin (50 nM; Calbiochem), PD98059 (50 μM ; Sigma-Aldrich), GW5074 (20 μM ; Sigma-Aldrich), LY94002 (25 μM ; Sigma-Aldrich) or SP60025 (20 μM ; Sigma-Aldrich). Medium was changed every 2-3 days. After at least 72 hours, cells were stimulated as indicated and target gene expression was assayed by RT-qPCR or western blotting.

HDAC inhibition

Subconfluent cells were cultured in presence of a dilution series of entinostat (MS-175; 40, 20, 10 and 2 μM ; Selleckchem BioConnect), vorinostat (suberoylanilide hydroxamic acid (SAHA); 10, 5 and 1 μM ; Sigma-Aldrich), trichostatin A (TSA; 5, 1 and 0.333 μM ; Sigma-Aldrich) or Sodium Butyrate (NaBu; 10, 5 and 1 mM; Sigma-Aldrich) in respective complete growth medium over night. Medium was changed for respective complete growth medium, cells were stimulated as indicated and target gene expression was assayed by RT-qPCR or western blotting. Since treatment with 10 μM entinostat showed a good increase in RelA K310 acetylation without signs of toxicity, subsequent experiments were performed using this dose.

Migration assays

(HPV-positive) KCs were stimulated as indicated for 24 hours. Cleared (HPV-positive) KC supernatants were added to the lower compartment of a transwell plate (Corning). The upper compartment was filled with peripheral blood mononuclear cells (PBMCs) isolated from buffy coats (Sanquin). PBMCs were allowed to migrate for 16 hours, after which the cells in the lower compartment were counted by flow cytometry in the presence of counting beads (Invitrogen) according to the manufacturer's instructions. Myeloid cells and lymphocytes were differentiated by their respective size in the FSC/SSC plot (data not shown).

RNA expression analyses and ELISA

The microarray data¹² is accessible in the Gene Expression Omnibus database (accession number GSE54181). Plots were generated using the

webtool R2: microarray analysis and visualization platform (<http://r2.amc.nl>).

Total RNA was isolated using the NucleoSpin RNA II kit (Machery-Nagel, Leiden, The Netherlands) according to the manufacturer's instructions. Total RNA (0.5–1.0 µg) was reverse transcribed using the SuperScript III First Strand synthesis system from Invitrogen. TaqMan PCR was performed using TaqMan Universal PCR Master Mix and pre-designed, pre-optimized primers and probe mix for CCL2, RANTES (CCL5), IL8 (CXCL8), CXCL9 and GAPDH (Applied Biosystems, Foster City, USA). Threshold cycle numbers (Ct) were determined using the CFX PCR System (BioRad, Veenendaal, The Netherlands) and the relative quantities of cDNA per sample were calculated using the $\Delta\Delta C_t$ method using GAPDH as the calibrator gene.

ELISA's for CCL2, RANTES, IL8 and CXCL9 were performed according to the manufacturer's instruction (PeproTech, London, United Kingdom).

Flow cytometry

Expression of EGFR on keratinocytes was analyzed by flow cytometry using PE-coupled Mouse-anti-human EGFR (1:20, BD Biosciences, Breda, The Netherlands). Per live gate, 50.000 cells were recorded using the BD FACS Calibur with Cellquest software (BD Bioscience) and data were analyzed using Flowjo (Treestar, Olten, Switzerland).

Western blot analysis

For Western blotting, polypeptides were resolved by SDS–polyacrylamide gel electrophoresis (SDS–PAGE) and transferred to a nitrocellulose membrane (Bio-Rad, Veenendaal, The Netherlands). Immunodetection was achieved with anti-p65 (1:1000, sc-372, Santa Cruz), anti-phospho-p65 (Ser536; 1:1000, #3033 Cell Signaling Technology (CST)), anti-acetyl-p65 (Lys310; 1:1000, #3045 CST), anti-IFRD1 (1:400, T2576 Sigma-Aldrich), β -actin (1:10,000, Sigma-Aldrich) primary antibodies, and HRP-coupled anti-mouse (1:5000; CST) and HRP-coupled anti-rabbit (1:5000, CST) secondary antibodies. Chemoluminescence reagent (Bio-Rad) was used as substrate and signal was scanned using the Chemidoc and accompanying Software (Bio-Rad) to quantify the intensity of the bands as a measure of the amount of protein of interest in the blot. The relative amount was determined by calculating the ratio of each protein over that of the density measured for the housekeeping protein β -actin.

Immunohistochemistry

4 µm formalin fixed, paraffin embedded tissue sections from two random VIN cases were deparaffinised and rehydrated using graded concentrations of ethanol to distilled water. Endogenous peroxidase activity was blocked with 0.03% H₂O₂/MeOH for 20 minutes. Antigen retrieval was performed in boiling EDTA buffer (pH 9.0) for 12 minutes. After 2 hours of cooling down to RT, slides were washed twice in distilled water and twice in phosphate-buffered saline (PBS). Subsequently, incubation was performed overnight at room temperature with the primary IFRD1 antibody (T2576 Sigma-Aldrich; 1:500 in PBS containing 1% bovine serum albumin); p16 (CINTEC, diluted 1:5) and E2 (1:50) (provided by Dr. F. Thierry). Second, sections were incubated with BrightVision polyhorseradish peroxidase anti-mouse/rabbit/rat IgG (Immunologic BV, Duiven, The Netherlands) for 30 minutes at room temperature. Washing between incubations was performed 3 times for 5 minutes in PBS. Immune complexes were visualized by applying a 0.05M tris-HCl buffer (pH 7.6) containing 0.05% of 3,3'-diamino-benzidine-tetrahydrochloride and 0.0018% of H₂O₂. After 10 minutes, the reaction was stopped by rinsing with demineralised water. Finally, the tissue sections were counterstained with Mayer's haematoxylin before addition of a cover slip.

Statistical analysis

Statistical analysis were performed using GraphPad InStat version 3.00. P-values were determined via Welch-corrected unpaired *t* tests. * *p*<0.05, ** *p*<0.01, *** *p*<0.001.

Conflict of interest

CM has received speaker honoraria from Merck, Quest Diagnostics, GSK, and Bristol-Myers. CM has performed research funded by Merck, The Phillip Morris External Research Program, NexMed, GSK, OriGenix, and Interferon Sciences Inc. Authors declare no other financial interests.

Author contributions

BT, RG, ESJ, CJMM, JMB and SHvdB designed the experiments. BT, RG, LPLP and ESJ performed the experiments. LPLP, EMGMvE and CM made viruses and cells. BT and SHvdB wrote the paper. CJMM, JMB and SHvdB supervised the project. All authors discussed the data.

Acknowledgements

This work was supported by the Netherlands Organization for Health Research (NOW/ZonMw) TOP grant 91209012. The funders had no role in study design, data collection and analysis, decision to publish, or preparation of the manuscript.

REFERENCES

1. Doorbar, J. *Molecular biology of human papillomavirus infection and cervical cancer. Clinical science* 110, 525-541, doi:10.1042/CS20050369 (2006).
2. Frazer, I. H. *Interaction of human papillomaviruses with the host immune system: a well evolved relationship. Virology* 384, 410-414, doi:10.1016/j.virol.2008.10.004 (2009).
3. Karim, R. et al. *Human papillomavirus deregulates the response of a cellular network comprising of chemotactic and proinflammatory genes. PLoS one* 6, e17848, doi:10.1371/journal.pone.0017848 (2011).
4. Richardson, H. et al. *The natural history of type-specific human papillomavirus infections in female university students. Cancer epidemiology, biomarkers & prevention : a publication of the American Association for Cancer Research, cosponsored by the American Society of Preventive Oncology* 12, 485-490 (2003).
5. van der Burg, S. H. & Melief, C. J. *Therapeutic vaccination against human papilloma virus induced malignancies. Current opinion in immunology* 23, 252-257, doi:10.1016/j.coi.2010.12.010 (2011).
6. zur Hausen, H. *Papillomaviruses and cancer: from basic studies to clinical application. Nature reviews. Cancer* 2, 342-350, doi:10.1038/nrc798 (2002).
7. Hasan, U. A. et al. *TLR9 expression and function is abolished by the cervical cancer-associated human papillomavirus type 16. Journal of immunology* 178, 3186-3197 (2007).
8. Karim, R. et al. *Human papillomavirus (HPV) upregulates the cellular deubiquitinase UCHL1 to suppress the keratinocyte's innate immune response. PLoS pathogens* 9, e1003384, doi:10.1371/journal.ppat.1003384 (2013).
9. Reiser, J. et al. *High-risk human papillomaviruses repress constitutive kappa interferon transcription via E6 to prevent pathogen recognition receptor and antiviral-gene expression. Journal of virology* 85, 11372-11380, doi:10.1128/JVI.05279-11 (2011).
10. Sunthamala, N. et al. *E2 proteins of high risk human papillomaviruses down-modulate STING and IFN-kappa transcription in keratinocytes. PLoS one* 9, e91473, doi:10.1371/journal.pone.0091473 (2014).
11. Termini, L. et al. *Characterization of global transcription profile of normal and HPV-immortalized keratinocytes and their response to TNF treatment. BMC medical genomics* 1, 29, doi:10.1186/1755-8794-1-29 (2008).
12. Tummers, B. et al. *CD40-Mediated Amplification of Local Immunity by Epithelial Cells Is Impaired by HPV. The Journal of investigative dermatology*, doi:10.1038/jid.2014.262 (2014).
13. Chang, Y. E. & Laimins, L. A. *Microarray analysis identifies interferon-inducible genes and*

- Stat-1 as major transcriptional targets of human papillomavirus type 31. Journal of virology* 74, 4174-4182 (2000).
14. Hong, S., Mehta, K. P. & Laimins, L. A. Suppression of STAT-1 expression by human papillomaviruses is necessary for differentiation-dependent genome amplification and plasmid maintenance. *Journal of virology* 85, 9486-9494, doi:10.1128/JVI.05007-11 (2011).
 15. Nees, M. et al. Papillomavirus type 16 oncogenes downregulate expression of interferon-responsive genes and upregulate proliferation-associated and NF-kappaB-responsive genes in cervical keratinocytes. *Journal of virology* 75, 4283-4296, doi:10.1128/JVI.75.9.4283-4296.2001 (2001).
 16. Zhou, F., Chen, J. & Zhao, K. N. Human papillomavirus 16-encoded E7 protein inhibits IFN-gamma-mediated MHC class I antigen presentation and CTL-induced lysis by blocking IRF-1 expression in mouse keratinocytes. *The Journal of general virology* 94, 2504-2514, doi:10.1099/vir.0.054486-0 (2013).
 17. Chen, L. F. & Greene, W. C. Shaping the nuclear action of NF-kappaB. *Nature reviews. Molecular cell biology* 5, 392-401, doi:10.1038/nrm1368 (2004).
 18. Conway, M. J. & Meyers, C. Replication and assembly of human papillomaviruses. *Journal of dental research* 88, 307-317, doi:10.1177/0022034509333446 (2009).
 19. McLaughlin-Drubin, M. E., Christensen, N. D. & Meyers, C. Propagation, infection, and neutralization of authentic HPV16 virus. *Virology* 322, 213-219, doi:10.1016/j.virol.2004.02.011 (2004).
 20. Meyers, C., Mayer, T. J. & Ozburn, M. A. Synthesis of infectious human papillomavirus type 18 in differentiating epithelium transfected with viral DNA. *Journal of virology* 71, 7381-7386 (1997).
 21. Lee, D., Lee, B., Kim, J., Kim, D. W. & Choe, J. cAMP response element-binding protein-binding protein binds to human papillomavirus E2 protein and activates E2-dependent transcription. *The Journal of biological chemistry* 275, 7045-7051 (2000).
 22. Quinlan, E. J., Culleton, S. P., Wu, S. Y., Chiang, C. M. & Androphy, E. J. Acetylation of conserved lysines in bovine papillomavirus E2 by p300. *Journal of virology* 87, 1497-1507, doi:10.1128/JVI.02771-12 (2013).
 23. Gu, Y. et al. Identification of IFRD1 as a modifier gene for cystic fibrosis lung disease. *Nature* 458, 1039-1042, doi:10.1038/nature07811 (2009).
 24. Micheli, L. et al. PC4/Tis7/IFRD1 stimulates skeletal muscle regeneration and is involved in myoblast differentiation as a regulator of MyoD and NF-kappaB. *The Journal of biological chemistry* 286, 5691-5707, doi:10.1074/jbc.M110.162842 (2011).
 25. Xue, Y. et al. HPV16 E2 is an immediate early marker of viral infection, preceding E7 expression in precursor structures of cervical carcinoma. *Cancer research* 70, 5316-5325,

- doi:10.1158/0008-5472.CAN-09-3789 (2010).
26. von Knebel Doeberitz, M., Gissmann, L. & zur Hausen, H. Growth-regulating functions of human papillomavirus early gene products in cervical cancer cells acting dominant over enhanced epidermal growth factor receptor expression. *Cancer research* 50, 3730-3736 (1990).
 27. Vietor, I. & Huber, L. A. Role of TIS7 family of transcriptional regulators in differentiation and regeneration. *Differentiation; research in biological diversity* 75, 891-897, doi:10.1111/j.1432-0436.2007.00205.x (2007).
 28. Kim, M. K. et al. Human papillomavirus type 16 E5 oncoprotein as a new target for cervical cancer treatment. *Biochemical pharmacology* 80, 1930-1935, doi:10.1016/j.bcp.2010.07.013 (2010).
 29. Bruzzese, F. et al. HDAC inhibitor vorinostat enhances the antitumor effect of gefitinib in squamous cell carcinoma of head and neck by modulating ErbB receptor expression and reverting EMT. *Journal of cellular physiology* 226, 2378-2390, doi:10.1002/jcp.22574 (2011).
 30. Liu, N. et al. Blocking the class I histone deacetylase ameliorates renal fibrosis and inhibits renal fibroblast activation via modulating TGF-beta and EGFR signaling. *PLoS one* 8, e54001, doi:10.1371/journal.pone.0054001 (2013).
 31. Heusinkveld, M. et al. M2 macrophages induced by prostaglandin E2 and IL-6 from cervical carcinoma are switched to activated M1 macrophages by CD4+ Th1 cells. *Journal of immunology* 187, 1157-1165, doi:10.4049/jimmunol.1100889 (2011).
 32. Feng, W., Duan, X., Liu, J., Xiao, J. & Brown, R. E. Morphoproteomic evidence of constitutively activated and overexpressed mTOR pathway in cervical squamous carcinoma and high grade squamous intraepithelial lesions. *International journal of clinical and experimental pathology* 2, 249-260 (2009).
 33. Kalinowski, A. et al. EGFR activation suppresses respiratory virus-induced IRF1-dependent CXCL10 production. *American journal of physiology. Lung cellular and molecular physiology* 307, L186-196, doi:10.1152/ajplung.00368.2013 (2014).
 34. Mascia, F., Mariani, V., Girolomoni, G. & Pastore, S. Blockade of the EGF receptor induces a deranged chemokine expression in keratinocytes leading to enhanced skin inflammation. *The American journal of pathology* 163, 303-312, doi:10.1016/S0002-9440(10)63654-1 (2003).
 35. Paul, T. et al. Cytokine regulation by epidermal growth factor receptor inhibitors and epidermal growth factor receptor inhibitor associated skin toxicity in cancer patients. *European journal of cancer* 50, 1855-1863, doi:10.1016/j.ejca.2014.04.026 (2014).
 36. Pastore, S. et al. ERK1/2 regulates epidermal chemokine expression and skin inflammation. *Journal of immunology* 174, 5047-5056 (2005).
 37. Vandermark, E. R. et al. Human papillomavirus type 16 E6 and E 7 proteins alter NF-

- κB* in cultured cervical epithelial cells and inhibition of NF-κB promotes cell growth and immortalization. *Virology* 425, 53-60, doi:10.1016/j.virol.2011.12.023 (2012).
38. Caberg, J. H. et al. Increased migration of Langerhans cells in response to HPV16 E6 and E7 oncogene silencing: role of CCL20. *Cancer immunology, immunotherapy : CII* 58, 39-47, doi:10.1007/s00262-008-0522-5 (2009).
 39. Havard, L., Rahmouni, S., Boniver, J. & Delvenne, P. High levels of p105 (NFκB1) and p100 (NFκB2) proteins in HPV16-transformed keratinocytes: role of E6 and E7 oncoproteins. *Virology* 331, 357-366, doi:10.1016/j.virol.2004.10.030 (2005).
 40. Avvakumov, N., Torchia, J. & Mymryk, J. S. Interaction of the HPV E7 proteins with the pCAF acetyltransferase. *Oncogene* 22, 3833-3841, doi:10.1038/sj.onc.1206562 (2003).
 41. Bernat, A., Avvakumov, N., Mymryk, J. S. & Banks, L. Interaction between the HPV E7 oncoprotein and the transcriptional coactivator p300. *Oncogene* 22, 7871-7881, doi:10.1038/sj.onc.1206896 (2003).
 42. Huang, S. M. & McCance, D. J. Down regulation of the interleukin-8 promoter by human papillomavirus type 16 E6 and E7 through effects on CREB binding protein/p300 and P/CAF. *Journal of virology* 76, 8710-8721 (2002).
 43. Spitkovsky, D., Hehner, S. P., Hofmann, T. G., Moller, A. & Schmitz, M. L. The human papillomavirus oncoprotein E7 attenuates NF-κB activation by targeting the IκB kinase complex. *The Journal of biological chemistry* 277, 25576-25582, doi:10.1074/jbc.M201884200 (2002).
 44. Hasan, U. A. et al. The human papillomavirus type 16 E7 oncoprotein induces a transcriptional repressor complex on the Toll-like receptor 9 promoter. *The Journal of experimental medicine* 210, 1369-1387, doi:10.1084/jem.20122394 (2013).
 45. Bodily, J. M., Mehta, K. P. & Laimins, L. A. Human papillomavirus E7 enhances hypoxia-inducible factor 1-mediated transcription by inhibiting binding of histone deacetylases. *Cancer research* 71, 1187-1195, doi:10.1158/0008-5472.CAN-10-2626 (2011).
 46. Hiscott, J., Nguyen, T. L., Arguello, M., Nakhaei, P. & Paz, S. Manipulation of the nuclear factor-κB pathway and the innate immune response by viruses. *Oncogene* 25, 6844-6867, doi:10.1038/sj.onc.1209941 (2006).
 47. Le Negrate, G. Viral interference with innate immunity by preventing NF-κB activity. *Cellular microbiology* 14, 168-181, doi:10.1111/j.1462-5822.2011.01720.x (2012).
 48. Ning, Z. et al. The N terminus of orf virus-encoded protein 002 inhibits acetylation of NF-κB p65 by preventing Ser(276) phosphorylation. *PLoS one* 8, e58854, doi:10.1371/journal.pone.0058854 (2013).
 49. Granja, A. G., Sabina, P., Salas, M. L., Fresno, M. & Revilla, Y. Regulation of inducible nitric oxide synthase expression by viral A238L-mediated inhibition of p65/RelA acetylation and p300 transactivation. *Journal of virology* 80, 10487-10496, doi:10.1128/JVI.00862-06 (2006).

SUPPLEMENTARY INFORMATION

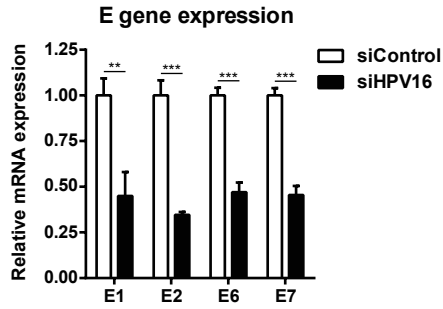


Figure S1: HPV16 E gene expression after HPV16 knock-down in HPV16+ KCs
*E1, E2, E6 and E7 expression in HFK16 cells transfected with siControl or siHPV16. Error bars indicate SD. P-values were determined via Welch-corrected unpaired t tests. ** $p < 0.01$, *** $p < 0.001$*

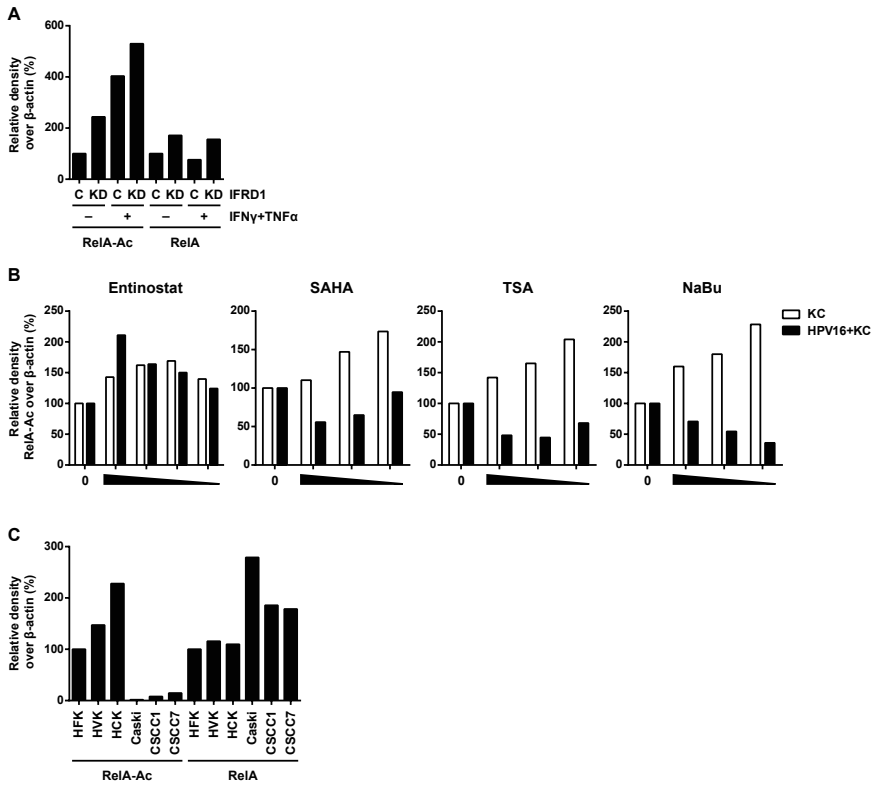


Figure S2: Western blot quantifications of RelA acetylation

(A) Quantified protein levels of RelA K310 acetylation and RelA over β -Actin in 24 hours non- or IFN γ and TNF α -stimulated control or IFRD1 knock-down (KD) HPV16+ KCs. The expression levels of the control-treated HPV16+ KCs were set as 100%.

(B) Quantified protein levels of RelA K310 acetylation over β -Actin in KCs and HPV16+ KCs treated with decreasing doses of entinostat (40, 20, 10 and 2 μ M), SAHA (10, 5 and 1 μ M), TSA (5, 1 and 0.333 μ M) or NaBu (10, 5 and 1 mM) (western blot Figure 4A).

The expression levels of the control-treated HPV16+ KCs were set as 100%.

(C) Quantified protein levels of RelA K310 acetylation and RelA over β -Actin in three KC donors and three HPV16-induced CxCa lines.

The expression levels of the HFK were set as 100%.

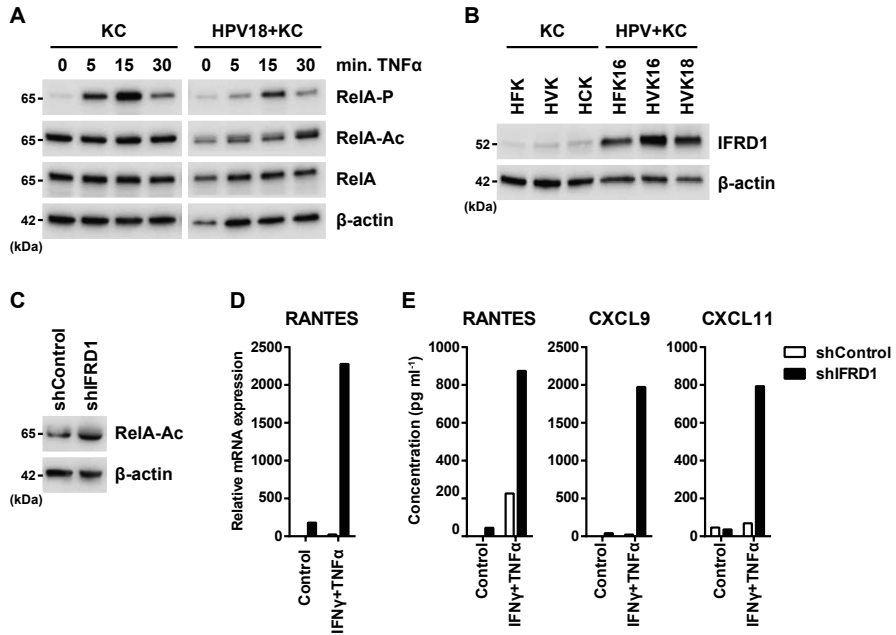


Figure S3: RelA acetylation, IFRD1 expression and IFRD1 knock-down effects in HPV18+ KCs

(A) RelA phosphorylation, acetylation and total levels in KCs and HPV18+ KCs stimulated with TNF α for 0, 5, 15 and 30 minutes.

(B) IFRD1 levels in three KC donor pools, two HPV16+ KC lines and one HPV18+ KC line.

(C) RelA acetylation levels in control or IFRD1 knock-down HPV18+ KCs.

(D) RT-qPCR of RANTES expression in 24 hours non- or IFN γ and TNF α -stimulated control or IFRD1 knock-down HPV18+ KCs.

(E) ELISA for RANTES, CXCL9 and CXCL11 in cleared supernatants of 24 hours non- or IFN γ and TNF α -stimulated control or IFRD1 knock-down HPV18+ KCs.

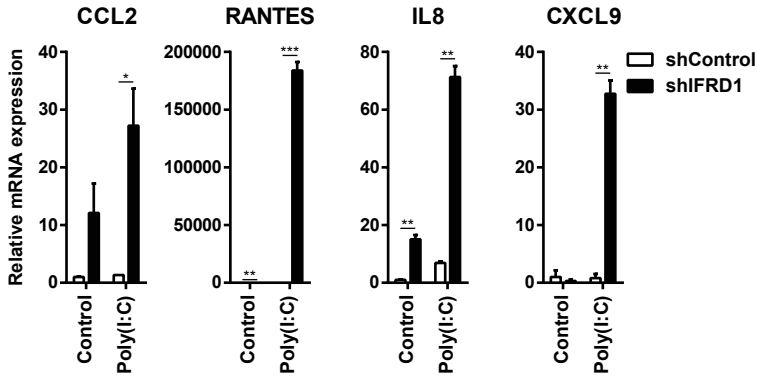
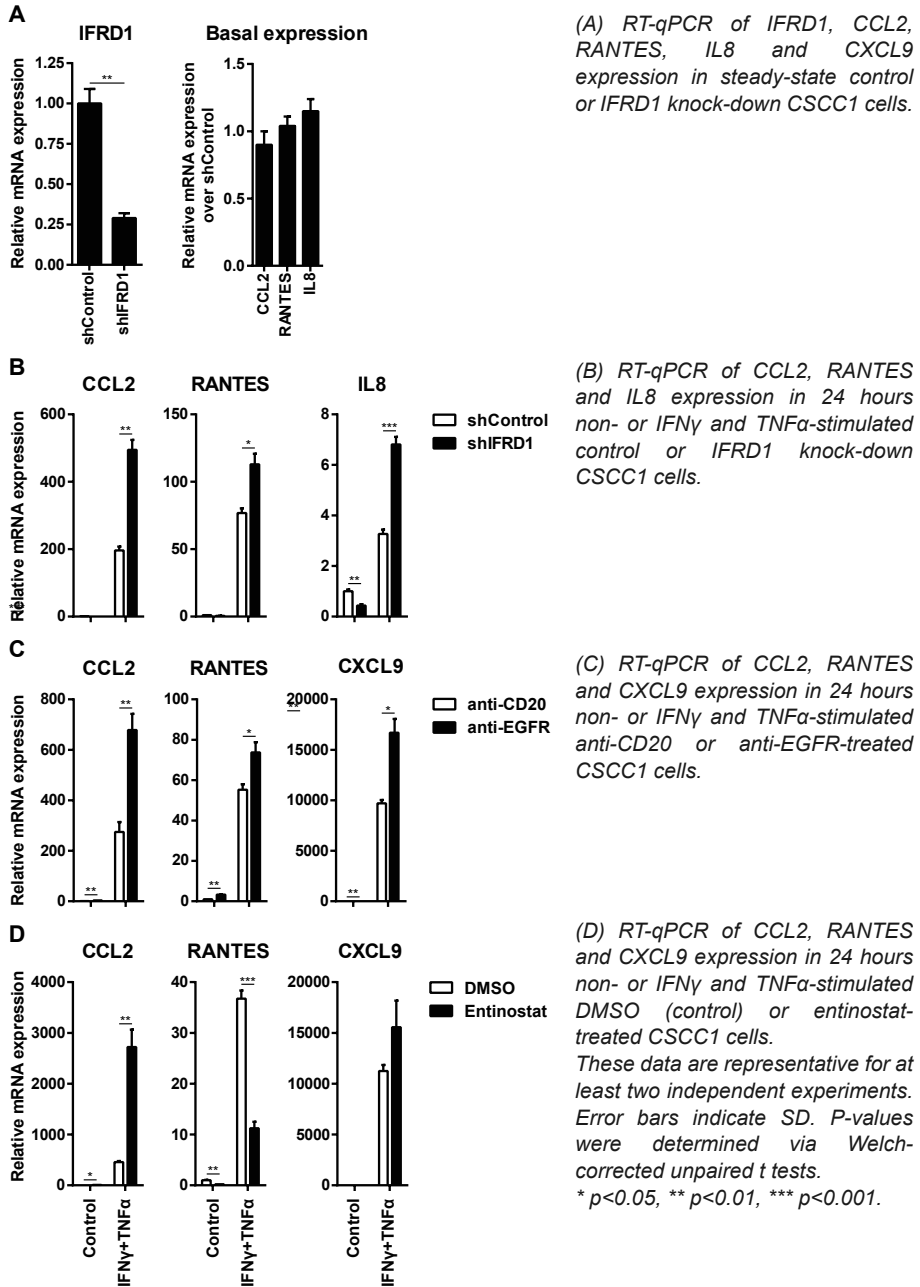


Figure S4: IFRD1 impairs Poly(I:C)-induced cytokine expression

RT-qPCR of CCL2, RANTES, IL8 and CXCL9 expression in 24 hours non- or Poly(I:C)-stimulated control or IFRD1 knock-down HPV16+ KCs.

These data are representative for at least two independent experiments. Error bars indicate SD. P-values were determined via Welch-corrected unpaired t tests. * $p < 0.05$, ** $p < 0.01$, *** $p < 0.001$.

Figure S5: The effects of IFRD1 knock-down, anti-EGFR and entinostat on CSCC1



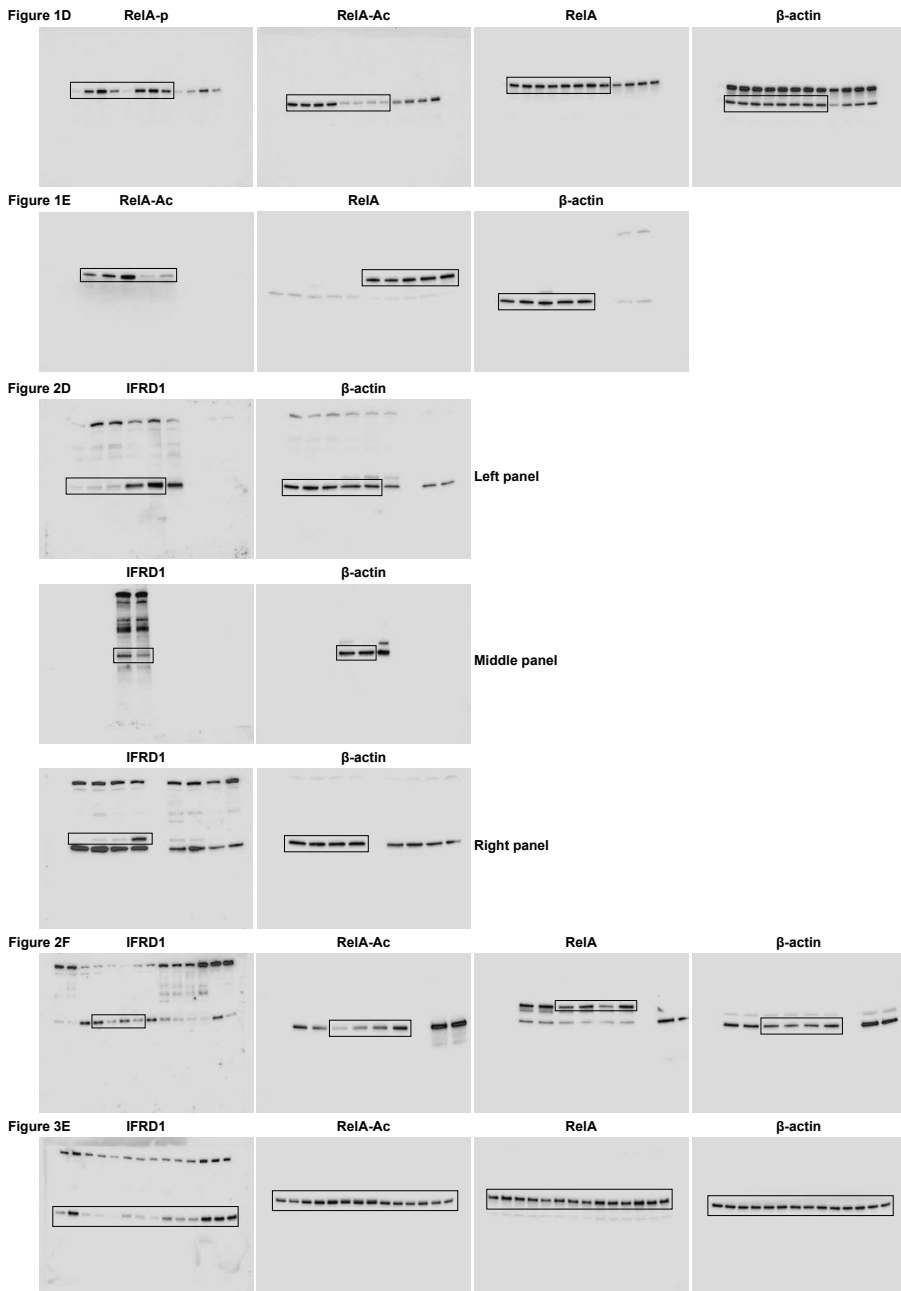


Figure S6: Full Western Blot data

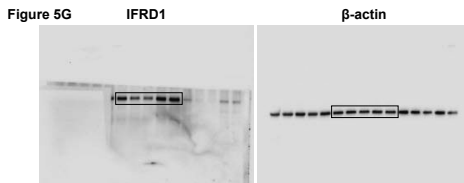
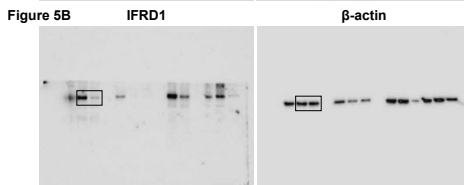
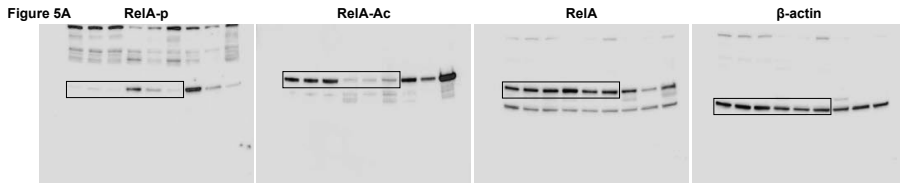
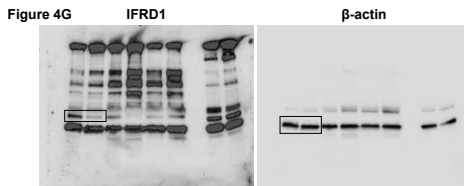
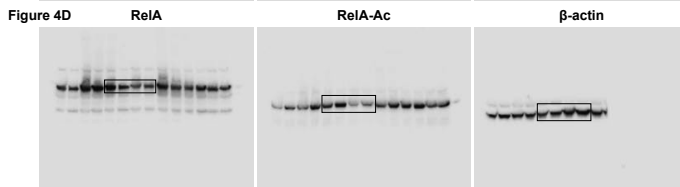
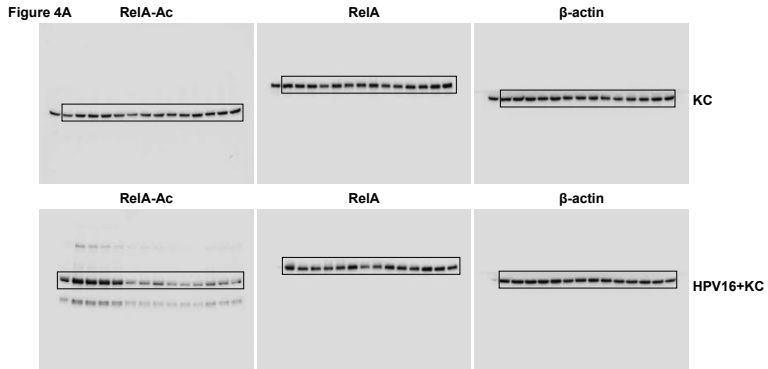


Figure S6: Full Western Blot data *Continued*

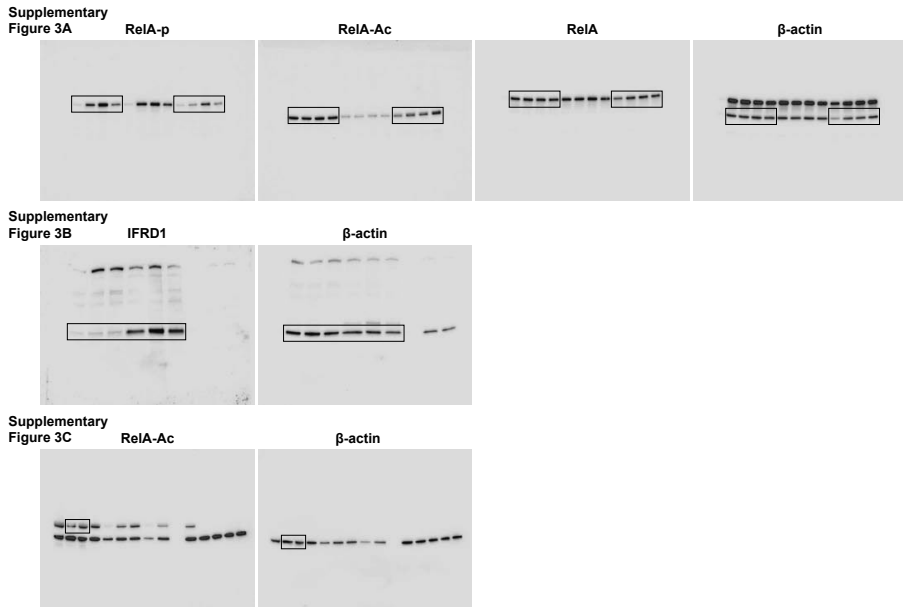


Figure S6: Full Western Blot data *Continued*
The full blots for all Western blot pictures. Above the blot the used target is indicated. The black boxes represent the depicted parts of the blot.

